



# Hexapartite steering based on a four-wave-mixing process with a spatially structured pump

YUNYUN LIANG,<sup>1,2</sup>  RONGGUO YANG,<sup>1,2,3,4</sup> JING ZHANG,<sup>1,2,3,\*</sup>   
AND TIANCAI ZHANG<sup>1,3</sup>

<sup>1</sup>State Key Laboratory of Quantum Optics and Quantum Optics Devices, Shanxi University, Taiyuan 030006, China

<sup>2</sup>College of Physics and Electronic Engineering, Shanxi University, Taiyuan 030006, China

<sup>3</sup>Collaborative Innovation Center of Extreme Optics, Shanxi University, Taiyuan, 030006, China

<sup>4</sup>yrg@sxu.edu.cn

\*zjj@sxu.edu.cn

**Abstract:** Multipartite Einstein-Podolsky-Rosen (EPR) steering has been widely studied, for realizing safer quantum communication. The steering properties of six spatially separated beams from the four-wave-mixing process with a spatially structured pump are investigated. Behaviors of all  $(1+i)/(i+1)$ -mode ( $i=1,2,3$ ) steerings are understandable, if the role of the corresponding relative interaction strengths are taken into account. Moreover, stronger collective multipartite steerings including five modes can be obtained in our scheme, which has potential applications in ultra-secure multiuser quantum networks when the issue of trust is critical. By further discussing about all monogamy relations, it is noticed that the type-IV monogamy relations, which are naturally included in our model, are conditionally satisfied. Matrix representation is used to express the steerings for the first time, which is very useful to understand the monogamy relations intuitively. Different steering properties obtained in this compact phase-insensitive scheme have potential applications for different kinds of quantum communication tasks.

© 2023 Optica Publishing Group under the terms of the [Optica Open Access Publishing Agreement](#)

## 1. Introduction

Quantum correlation is one of the central concepts in quantum information theory [1], and there is often a clear hierarchy among different correlations, which includes total correlation, discord, entanglement, steering, and Bell nonlocality [2]. Einstein-Podolsky-Rosen (EPR) steering [3], which was first proposed by Schrödinger in 1935 [4] and developed with concrete definition and criterion by Wiseman in 2007 [5,6], denotes a quantum correlation situated between entanglement and Bell nonlocality, i.e., EPR steering is stricter than quantum entanglement. It is identified as a significant physical resource for one-sided device-independent (1SDI) quantum key distribution [7,8], secure quantum teleportation [9,10], and subchannel discrimination [11], due to its natural asymmetry, which means that Alice's ability to steer Bob may not be equal to Bob's ability to steer Alice. The situation that only one part can steer the other is called one-way steering [12,13], which has potential applications in hierarchical quantum communication. The situation that both parts can steer each other is called two-way steering, which was proved to achieve quantum teleportation with fidelity greater than 0.67 [10]. Besides bipartite steering, multipartite steering was also defined [14] and the corresponding criterion was given theoretically [15] and then verified experimentally [16]. Multipartite steering, which is important for scalable quantum network, can be generated in many physical systems, such as cavity optomechanical system [17–19], optical parametric process [20,21], and four-wave mixing (FWM) system [22,23]. The four-wave mixing (FWM) process can be used to generate squeezed [24] or entangled state of light [25–27], and can be further generate multipartite entanglement when cascaded FWM is

applied [27,28]. Genuine tripartite steering, one-way steering, and collective steering based on asymmetric cascaded FWM structure were discussed [22,29]. Quadripartite steering generated from the symmetric and asymmetric cascaded FWM structures was demonstrated and four distinct types of monogamy relations were analyzed accordingly [23]. By adding one more FWM, pentapartite steering can be obtained and collective multipartite steering can only exist in the asymmetry structure when optical loss is considered [30]. To achieve better scalability, FWM process with a spatially structured pump (SSP) [31–34], which can be realized by altering the angle between two or more pump beams, was adopted to generate quantum correlations among six [22], ten [35], fourteen [36] output beams experimentally. Besides scalability, using spatially structured pump can make the experimental setup simpler and compacter. In this paper, we investigate the steering ability of six spatially separated output beams from a FWM process with a spatially structured pump [37], and demonstrate the corresponding  $(1+i)/(i+1)$ -mode ( $i=1,2,3$ ) steerings, collective steerings, and monogamy relations.

## 2. Physical model and theoretical derivation

We consider a FWM process with a spatially structured pump, as is shown in Fig. 1(a). Two bright pump beams (pump1 and pump2) and a weak seed beam are focused in the center of the  $^{85}\text{Rb}$  vapor cell with a small tilted angle. Three probe beams ( $\hat{a}_2, \hat{a}_3, \hat{a}_4$ ) and three conjugate beams ( $\hat{a}_1, \hat{a}_5, \hat{a}_6$ ) are simultaneously generated and naturally separated in space. The corresponding atomic energy level diagram is shown in Fig. 1(b). According to the phase-matching conditions, single-pump and double-pump FWM processes both happen. Therefore, correlations between  $\hat{a}_1$  and  $\hat{a}_2$ ,  $\hat{a}_3$  and  $\hat{a}_5$ ,  $\hat{a}_1$  and  $\hat{a}_4$ ,  $\hat{a}_3$  and  $\hat{a}_6$ , are generated through single-pumped processes, and correlations between  $\hat{a}_1$  and  $\hat{a}_3$ ,  $\hat{a}_4$  and  $\hat{a}_5$ ,  $\hat{a}_2$  and  $\hat{a}_6$ , are generated through double-pumped processes, which can be seen in Fig. 1(c). The interaction Hamiltonian can be written as

$$\hat{H} = i\hbar[\varepsilon_1\hat{a}_1^\dagger\hat{a}_2^\dagger + \varepsilon_2\hat{a}_1^\dagger\hat{a}_3^\dagger + \varepsilon_3\hat{a}_1^\dagger\hat{a}_4^\dagger + \varepsilon_4\hat{a}_3^\dagger\hat{a}_5^\dagger + \varepsilon_5\hat{a}_3^\dagger\hat{a}_6^\dagger + \varepsilon_6\hat{a}_4^\dagger\hat{a}_5^\dagger + \varepsilon_7\hat{a}_2^\dagger\hat{a}_6^\dagger] + H.c. \quad (1)$$

where  $\hat{a}_1^\dagger, \dots, \hat{a}_6^\dagger$  are the creation operators of six output beams. The first and forth terms represents the FWM processes of generating  $\hat{a}_1$  and  $\hat{a}_2$ ,  $\hat{a}_3$  and  $\hat{a}_5$  with a single pump (pump1). The third and fifth terms represents the generation of  $\hat{a}_1$  and  $\hat{a}_4$ ,  $\hat{a}_3$  and  $\hat{a}_6$  through single-pump (pump2) FWM processes. The second, sixth, and seventh terms corresponds to the double-pump (pump1 and pump2) FWM processes of generating  $\hat{a}_1$  and  $\hat{a}_3$ ,  $\hat{a}_4$  and  $\hat{a}_5$ ,  $\hat{a}_2$  and  $\hat{a}_6$  beams.  $\varepsilon_1 \dots \varepsilon_7$  represents the interaction strengths of seven different FWM processes. H.c. means the Hermitian conjugate. Considering the symmetry of the output beams, we assume that  $\varepsilon_1 = \varepsilon_4 = G_1$  (pump1),  $\varepsilon_3 = \varepsilon_5 = G_2$  (pump2),  $\varepsilon_2 = \varepsilon_6 = \varepsilon_7 = G_3$  (double pumps), to make it convenient to calculate and understand. According to the Hamiltonian shown in Eq. (1), the Heisenberg equations governing the time evolution of the six output beams ( $\hat{a}_1, \dots, \hat{a}_6$ ) can be obtained as,

$$\begin{aligned} \frac{d\hat{a}_1}{dt} &= \varepsilon_1\hat{a}_2^\dagger + \varepsilon_2\hat{a}_3^\dagger + \varepsilon_3\hat{a}_4^\dagger \\ \frac{d\hat{a}_2}{dt} &= \varepsilon_1\hat{a}_1^\dagger + \varepsilon_2\hat{a}_6^\dagger \\ \frac{d\hat{a}_3}{dt} &= \varepsilon_2\hat{a}_1^\dagger + \varepsilon_1\hat{a}_5^\dagger + \varepsilon_3\hat{a}_6^\dagger \\ \frac{d\hat{a}_4}{dt} &= \varepsilon_3\hat{a}_1^\dagger + \varepsilon_2\hat{a}_5^\dagger \\ \frac{d\hat{a}_5}{dt} &= \varepsilon_1\hat{a}_3^\dagger + \varepsilon_2\hat{a}_4^\dagger \\ \frac{d\hat{a}_6}{dt} &= \varepsilon_2\hat{a}_2^\dagger + \varepsilon_3\hat{a}_3^\dagger, \end{aligned} \quad (2)$$

where the coefficients in Eq. (2) can be expressed by matrix  $A$ ,

$$A = \begin{pmatrix} 0 & \varepsilon_1 & \varepsilon_2 & \varepsilon_3 & 0 & 0 \\ \varepsilon_1 & 0 & 0 & 0 & 0 & \varepsilon_2 \\ \varepsilon_2 & 0 & 0 & 0 & \varepsilon_1 & \varepsilon_3 \\ \varepsilon_3 & 0 & 0 & 0 & \varepsilon_2 & 0 \\ 0 & 0 & \varepsilon_1 & \varepsilon_2 & 0 & 0 \\ 0 & \varepsilon_2 & \varepsilon_3 & 0 & 0 & 0 \end{pmatrix}. \quad (3)$$

Based on the definitions of the quadrature amplitude operators  $\hat{X}_i$  and quadrature phase operators  $\hat{Y}_i$ ,  $\hat{X}_i = (\hat{a}_i + \hat{a}_i^\dagger)/\sqrt{2}$  and  $\hat{Y}_i = i(\hat{a}_i^\dagger - \hat{a}_i)/\sqrt{2}$ , the corresponding Heisenberg equations can be written in matrix form

$$\frac{d\xi}{dt} = G\xi, \quad (4)$$

where  $\xi = (\hat{X}_1, \dots, \hat{X}_6, \hat{Y}_1, \dots, \hat{Y}_6)^T$ , and the coefficient matrix  $G$  can be expressed by  $G = \text{diag}[A, -A]$ . Then Eq. (4) can be solved by diagonalizing  $G$ , i.e.,  $G = PG_{\text{diag}}P^{-1}$ , and the solution can be expressed by  $\xi = S\xi(0)$ , where  $S$  is a symplectic matrix describing the relationship between the output and input beams and can be obtained by  $S = Pe^{G_{\text{diag}}t}P^{-1}$ . Therefore, the covariance matrix (CM) of the output six modes can be given by [38,39]

$$\sigma = \langle \xi \xi^T \rangle = S \langle \xi(0) \xi(0)^T \rangle S^T = SS^T \quad (5)$$

Based on the CM, the EPR steering properties between the output beams can be quantified by steering criterion. For a bipartite Gaussian state system ( subsystem A contains  $n_A$  modes and subsystem B contains  $n_B$  modes), the corresponding CM can be reconstructed in the form

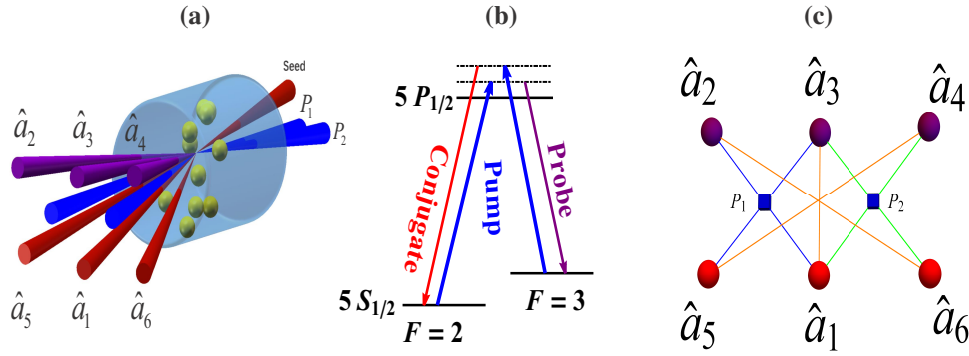
$$\sigma_{AB} = \begin{pmatrix} \mathcal{A} & C \\ C^T & \mathcal{B} \end{pmatrix}, \quad \text{where submatrices } \mathcal{A} \text{ and } \mathcal{B} \text{ are the reduced state of subsystem A and B,}$$

respectively, and submatrix  $C$  corresponds to the correlation between them. The steerability from subsystem A to subsystem B ( $A \rightarrow B$ ) and from subsystem B to subsystem A ( $B \rightarrow A$ ) can be defined as [40]

$$\mathcal{G}^{A \rightarrow B}(\sigma_{AB}) = \max \left\{ 0, - \sum_{j: \tilde{v}_j^{\mathcal{A}\mathcal{B}/\mathcal{A}} < 1} \ln(\tilde{v}_j^{\mathcal{A}\mathcal{B}/\mathcal{A}}) \right\} \quad (6)$$

$$\mathcal{G}^{B \rightarrow A}(\sigma_{BA}) = \max \left\{ 0, - \sum_{j: \tilde{v}_j^{\mathcal{A}\mathcal{B}/\mathcal{B}} < 1} \ln(\tilde{v}_j^{\mathcal{A}\mathcal{B}/\mathcal{B}}) \right\}. \quad (7)$$

where  $\tilde{v}_j^{\mathcal{A}\mathcal{B}/\mathcal{A}} (j = 1, \dots, n_B)$  and  $\tilde{v}_j^{\mathcal{A}\mathcal{B}/\mathcal{B}} (j = 1, \dots, n_A)$  are the symplectic eigenvalues of  $\tilde{\sigma}_{\mathcal{A}\mathcal{B}/\mathcal{A}} = \mathcal{B} - C^T \mathcal{A}^{-1} C$  and  $\tilde{\sigma}_{\mathcal{A}\mathcal{B}/\mathcal{B}} = \mathcal{A} - C^T \mathcal{B}^{-1} C$ , respectively. B can be steered by A if  $\mathcal{G}^{A \rightarrow B} > 0$ . A can be steered by B if  $\mathcal{G}^{B \rightarrow A} > 0$ . When  $(\mathcal{G}^{A \rightarrow B} > 0)$  and  $(\mathcal{G}^{B \rightarrow A} > 0)$  are both satisfied, the steering is two-way (A and B can steer each other), otherwise  $(\mathcal{G}^{A \rightarrow B} > 0, \mathcal{G}^{B \rightarrow A} = 0)$  or  $(\mathcal{G}^{B \rightarrow A} > 0, \mathcal{G}^{A \rightarrow B} = 0)$  represents a one-way steering (only A can steer B, or only B can steer A). This criterion is a sufficient and necessary condition for testing steering of Gaussian states with quadrature measurements, but it is not a necessary condition for a non-Gaussian scenario, although it still validates the presence of steering [23].

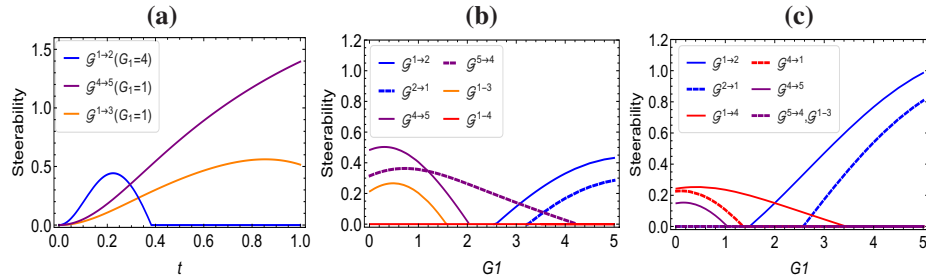


**Fig. 1.** The FWM process with a spatially structured pump. (a) Generated six beams after FWM process with structured pump1 ( $P_1$ ) and pump2 ( $P_2$ ). ( $\hat{a}_2, \hat{a}_3, \hat{a}_4$ ) and ( $\hat{a}_1, \hat{a}_5, \hat{a}_6$ ) are the probe and conjugate beams, respectively. (b) The corresponding energy-level diagram of the double- $\Lambda$  scheme in the D1 line of  $^{85}\text{Rb}$  vapor cell. (c) The output beams from the SSP based on FWM process. The purple and red balls represent the probe and conjugate beams, separately. The intersections of the blue, green, and orange lines correspond to pump1 ( $P_1$ ), pump2 ( $P_2$ ), and double pumps, separately.

### 3. $(1+i)/(i+1)$ -mode EPR steering

#### 3.1. $(1+1)$ -mode EPR steering

Figure 2(a) gives the time evolution of all  $(1+1)$ -mode steerings and shows that  $t = 0.3$  can make all these steerings considerable. The  $(1+1)$ -mode steerings versus the interaction strength  $G_1$  under different parameters are shown in Fig. 2(b) ( $G_2 = 1.2, G_3 = 2, t = 0.3$ ) and Fig. 2(c) ( $G_2 = 2, G_3 = 1.2, t = 0.3$ ), respectively.

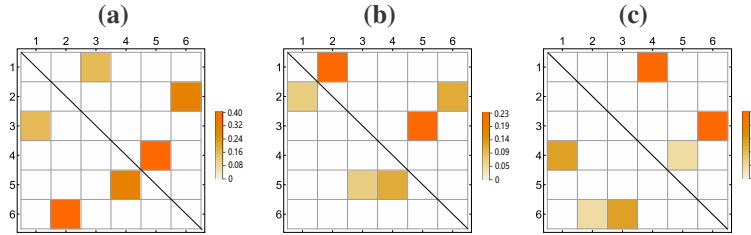


**Fig. 2.** The  $(1+1)$ -mode steerings. (a) The steerabilities versus the interaction time  $t$  when  $G_2 = 1.2, G_3 = 2$ . The  $(1+1)$ -mode steerings versus  $G_1$  for  $t = 0.3$ , (b) with  $G_2 = 1.2, G_3 = 2$ , and (c) with  $G_2 = 2, G_3 = 1.2$ .

It is clear that the  $(1+1)$ -mode steerings exist only between probe beams and conjugate beams, due to the direct interactions. According to the symmetry in Fig. 1(c),  $\mathcal{G}^{1 \rightarrow 2} = \mathcal{G}^{3 \rightarrow 5}$ ,  $\mathcal{G}^{1 \rightarrow 4} = \mathcal{G}^{3 \rightarrow 6}$ ,  $\mathcal{G}^{5 \rightarrow 4} = \mathcal{G}^{2 \rightarrow 6}$ , and vice versa. As is shown in Fig. 2(b), one-way or two-way steering sensitively depends on the corresponding interaction strength. Steering between optical modes  $\hat{a}_1$  and  $\hat{a}_3$  (mainly depend on the double-pump interaction strength  $G_3$ ) is always symmetric two-way steering, which can be well understood by their symmetry (both frequency and intensity), and will vanish when  $G_1$  is bigger than 1.6, i.e., the critical interaction strength  $G_1$  is between  $G_2$  and  $G_3$ , which means  $G_3$  should be stronger enough than the other two to obtain two-way steerings. For steering between  $\hat{a}_1$  and  $\hat{a}_2$ , there only exist one-way steering from  $\hat{a}_1$  to  $\hat{a}_2$  when  $2.6 < G_1 < 3.2$ , and two-way asymmetric steering between  $\hat{a}_1$  and  $\hat{a}_2$  will happen when  $G_1 > 3.2$ .

There exist a threshold because steering between  $\hat{a}_1$  and  $\hat{a}_2$  mainly depends on pump 1, which means  $G_1$  should be strong enough. It is also noticed that steering from  $\hat{a}_1$  to  $\hat{a}_2$  is always stronger than that from  $\hat{a}_2$  to  $\hat{a}_1$ , because all pump1, pump2 and double pump can affect mode  $\hat{a}_1$  but only two of them (pump1 and double pump) can affect  $\hat{a}_2$ . For steering between  $\hat{a}_4$  and  $\hat{a}_5$ , it mainly depends on double pump ( $G_3$ ), however,  $\hat{a}_4$  and  $\hat{a}_5$  are also affected by pump2 and pump1, respectively. Therefore, when  $G_1$  is small ( $<1.2$ ),  $\mathcal{G}^{4 \rightarrow 5} > \mathcal{G}^{5 \rightarrow 4}$ , and when  $G_1$  is bigger ( $>1.2$ ),  $\mathcal{G}^{4 \rightarrow 5} < \mathcal{G}^{5 \rightarrow 4}$ , and when  $G_1 > 2.1$  there only exist one-way steering from  $\hat{a}_5$  to  $\hat{a}_4$ . It is interesting that symmetric two-way steering will happen at the intersection point  $G_1 = 1.2$ . In Fig. 2(c), another parameters are chosen to show steerings between  $\hat{a}_1$  and  $\hat{a}_4$  clearly, which can be understood in the same way, and other steerings are also shown.

Specially, matrix diagram can be used to represent all these one-way and two-way steerings, as is shown in Fig. 3(a), Fig. 3(b) and Fig. 3(c), with different parameters, respectively. Matrix element  $A_{ij}$  represents the steering from  $i$  to  $j$  and different colors represent different steerabilities. Therefore, two-way steerings related to two elements that is symmetric to the diagonal line, while one-way steerings related to those elements that have no symmetric counterparts. For example, in Fig. 3(a), three two-way steerings are demonstrated, however, only steering between  $\hat{a}_1$  and  $\hat{a}_3$  is symmetric two-way (same color). This matrix representation can help us to demonstrate the steerings more intuitively. Furthermore, the satisfied type-I monogamy relations can also be found from these matrix representations, i.e., when  $\hat{a}_1$  can be steered by  $\hat{a}_3$ , it cannot be steered by other modes simultaneously, . . . . ., etc. Note that all the (1+1)-mode steerings can be reasonably explained by the relative interaction strengths, i.e., the direct interaction that dominate the (1+1)-mode steering should be strong enough compared with other interactions, to keep a considerable steerability. Moreover, the asymmetric two-way steering results from the asymmetric intensity. For example, the intensity of  $\hat{a}_1$  ( $\hat{a}_3$ ) is the strongest, therefore the steering from it to other mode is stronger than that from other mode to it.

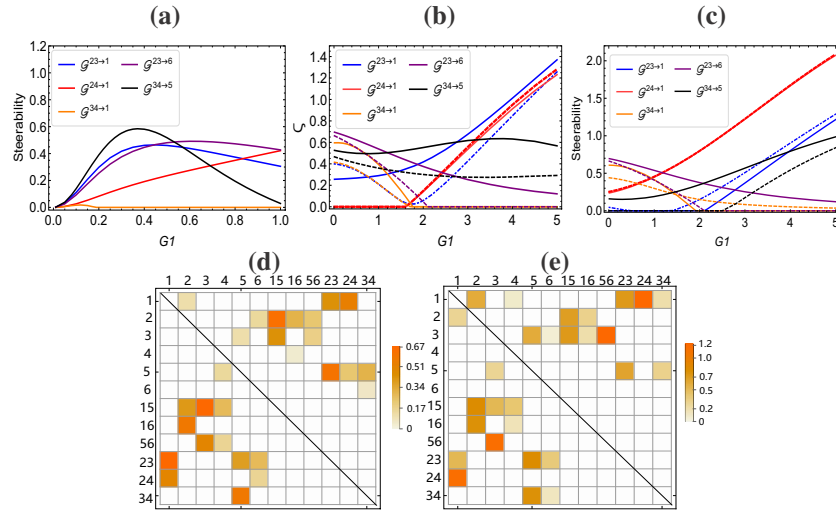


**Fig. 3.** Matrix representation of (1+1)-mode steerings. (a)  $G_1 = 1, G_2 = 1.2, G_3 = 2$ . (b)  $G_1 = 3.5, G_2 = 1.2, G_3 = 2$ . (c)  $G_1 = 1, G_2 = 2, G_3 = 1.2$ .

### 3.2. (1+2)/(2+1)-mode EPR steering

The (1+2)/(2+1)-mode steerings, which means the steered part or steering part contains two modes, are shown in Fig. 4.  $t = 0.3$  is chosen for consistency, according to Fig. 4(a).  $\mathcal{G}^{34 \rightarrow 5} = \mathcal{G}^{16 \rightarrow 2}$ ,  $\mathcal{G}^{23 \rightarrow 6} = \mathcal{G}^{15 \rightarrow 4}$ ,  $\mathcal{G}^{24 \rightarrow 1} = \mathcal{G}^{56 \rightarrow 3}$ ,  $\mathcal{G}^{23 \rightarrow 1} = \mathcal{G}^{15 \rightarrow 3}$ ,  $\mathcal{G}^{34 \rightarrow 1} = \mathcal{G}^{16 \rightarrow 3}$ , and vice versa, due to the symmetry in Fig. 1(c). As is shown in Fig. 4(b), steering between modes  $\hat{a}_2\hat{a}_3$  and mode  $\hat{a}_6$  will change from two-way to one-way when  $G_1 > 2.1$ , and steerings will decrease when  $G_1$  increase because they are mainly depend on the interaction strength  $G_2$  and  $G_3$ . For steering between modes  $\hat{a}_2\hat{a}_3$  and mode  $\hat{a}_1$  is always two-way, when  $G_1$  is small ( $<0.8$ ),  $\mathcal{G}^{1 \rightarrow 23} > \mathcal{G}^{23 \rightarrow 1}$ , and when  $G_1$  is bigger ( $>0.8$ ),  $\mathcal{G}^{1 \rightarrow 23} < \mathcal{G}^{23 \rightarrow 1}$ . It is interesting that symmetric two-way steering will happen at the intersection point  $G_1 = 0.8$ , and both steerings will increase when  $G_1$  is further increasing because they are mainly depend on  $G_1$  and  $G_3$ . Steering between modes  $\hat{a}_3\hat{a}_4$  and mode  $\hat{a}_5$  is always two-way due to strong  $G_3$ . Steering between modes  $\hat{a}_3\hat{a}_4$  and mode  $\hat{a}_1$  is

two-way and will vanish when  $G_1 > 1.8$  due to smaller relative strength of  $G_2$ . Steering between modes  $\hat{a}_2\hat{a}_4$  and mode  $\hat{a}_1$  has a smaller threshold compare with that between  $\hat{a}_2$  and  $\hat{a}_1$  (shown in Fig. 2(b)) due to the contribution of pump2. Results for bigger relative strength of  $G_2$  are shown in Fig. 4(c). In Fig. 4(c), Steering between modes  $\hat{a}_2\hat{a}_4$  and mode  $\hat{a}_1$  is always two-way due to stronger  $G_2$ . Steering between modes  $\hat{a}_3\hat{a}_4$  and mode  $\hat{a}_5$  will change from one-way to two-way  $G_1 > 2.5$ , due to smaller relative strength of  $G_3$  and initial weak  $G_1$ . Steering between modes  $\hat{a}_3\hat{a}_4$  and mode  $\hat{a}_1$  will change from two-way to one-way when  $G_1 > 1.9$  with a intersection of symmetric two-way steering at  $G_1 = 1.5$ . This is understandable: when  $G_1$  is further increased, steering between  $\hat{a}_1$  and  $\hat{a}_3$  vanishes due to smaller relative  $G_3$  and steering from  $\hat{a}_1$  to  $\hat{a}_4$  is stronger than that from  $\hat{a}_4$  to  $\hat{a}_1$  due to strong intensity of  $\hat{a}_1$ . Fig. 4(d) and Fig. 4(e) are the matrix representations under different parameters, which contain all possible  $(1+2)/(2+1)$  modes. From the matrix representations, it is found that the type-II monogamy relations also can be satisfied, for example, when  $\hat{a}_5$  can be steered by  $\hat{a}_2\hat{a}_3$ , it cannot be steered by  $\hat{a}_4$  simultaneously; when  $\hat{a}_1$  can be steered by  $\hat{a}_2\hat{a}_4$ , it cannot be steered by  $\hat{a}_3$  simultaneously; . . . . . Note that the  $(1+2)/(2+1)$ -mode steering depends on the superimposed effect of the corresponding  $(1+1)$ -mode steerings and is still sensitive to the relative interaction strength.

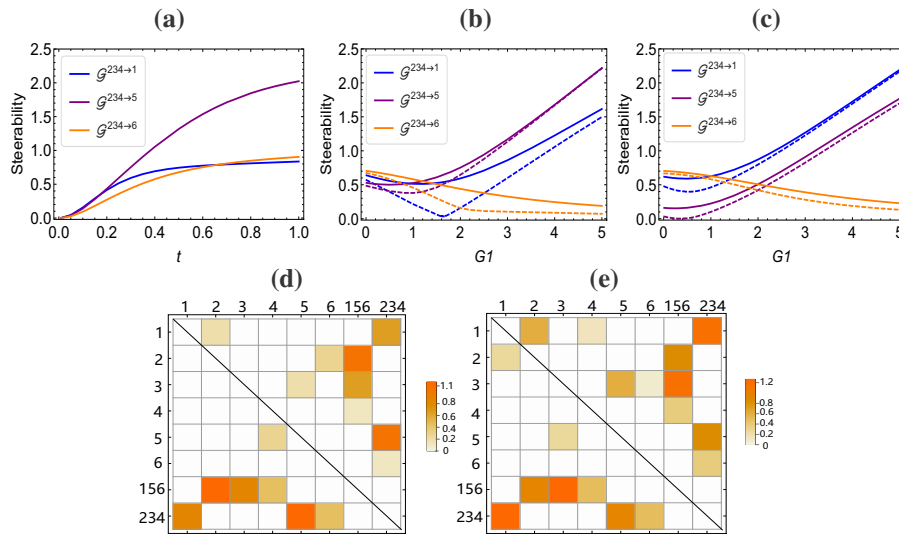


**Fig. 4.** Results of the  $(1+2)/(2+1)$ -mode steerings. (a) Time evolution, with  $G_1 = 2$ ,  $G_3 = 2$ ,  $G_2 = 1.2$ . (b) The steerings versus  $G_1$ ,  $G_2 = 1.2$ ,  $G_3 = 2$ . (c) The steerings versus  $G_1$ ,  $G_2 = 2$ ,  $G_3 = 1.2$ . In subgraph (b) and (c), the solid line and dashed line of the same color correspond to a pair of counterparts, for example, the solid and dashed blue lines correspond to  $\mathcal{G}^{23 \rightarrow 1}$  and  $\mathcal{G}^{1 \rightarrow 23}$ , respectively. (d) Matrix representation with  $G_2 = 1.2$ ,  $G_3 = 2$ ,  $G_1 = 3$ . (e) Matrix representation with  $G_2 = 2$ ,  $G_3 = 1.2$ ,  $G_1 = 3$ .

### 3.3. $(1+3)/(3+1)$ -mode EPR steering

The  $(1+3)/(3+1)$ -mode steerings are shown in Fig. 5.  $t=0.3$  is still chosen for consistency based on the time evolution diagram Fig. 5(a), and it is found that the steerabilities are robust and stronger when the steering part or the steered part contain three modes, because more correlations contribute to the steerings. Still we have  $\mathcal{G}^{234 \rightarrow 1} = \mathcal{G}^{156 \rightarrow 3}$ ,  $\mathcal{G}^{234 \rightarrow 5} = \mathcal{G}^{156 \rightarrow 2}$ ,  $\mathcal{G}^{234 \rightarrow 6} = \mathcal{G}^{156 \rightarrow 4}$ , and vice versa, due to the symmetry in Fig. 1(c). Specially, all  $(1+3)/(3+1)$ -mode steerings are asymmetric two-way, as is shown in Fig. 5(b) and Fig. 5(c). It means the more the steering or steered modes, the less dependence on the relative strength. However, bigger relative strength of  $G_2$  leads to stronger steering between modes  $\hat{a}_2\hat{a}_3\hat{a}_4$  and mode  $\hat{a}_1$ , compared

with that between  $\hat{a}_2\hat{a}_3\hat{a}_4$  and  $\hat{a}_5$ . With the increase of  $G_1$ ,  $\mathcal{G}^{1 \rightarrow 234}$  decrease, while  $\mathcal{G}^{234 \rightarrow 1}$  and  $\mathcal{G}^{234 \rightarrow 5}$  finally increase. Generally, steering from one-mode to multi-modes is smaller than that of multi-mode to one-mode, for example,  $\mathcal{G}^{234 \rightarrow 1} > \mathcal{G}^{1 \rightarrow 234}$  (The solid line is higher than the dashed line of the same color). It is clearly shown from the matrix representation in Fig. 5(d) and Fig. 5(e), all  $(1+3)/(3+1)$ -mode steerings are asymmetric two-way steerings. Moreover, from the matrix representations, it is found that the type-III monogamy relations can be satisfied, for example, the steerability  $\mathcal{G}^{156 \rightarrow 2}$  is bigger than the sum steerabilities  $\mathcal{G}^{1 \rightarrow 2}$ ,  $\mathcal{G}^{5 \rightarrow 2}$ , and  $\mathcal{G}^{6 \rightarrow 2}$ ; the steerability of  $\mathcal{G}^{2 \rightarrow 156}$  is bigger than the sum of steerabilities  $\mathcal{G}^{2 \rightarrow 1}$ ,  $\mathcal{G}^{2 \rightarrow 5}$ , and  $\mathcal{G}^{2 \rightarrow 6}$ ; . . . . . Note that the  $(1+3)/(3+1)$ -mode steering is not so sensitive to the relative interaction strength any more, because the indirect interactions work and then the interaction strengths  $G_1$ ,  $G_2$  and  $G_3$  are all included. By the way, when more modes ( $>3$ ) are considered, the joint steering of more modes is always bigger than that of less modes.



**Fig. 5.** The  $(1+3)/(3+1)$ -mode steerings. (a) The time evolution diagram with  $G_1 = 2$ ,  $G_3 = 2$ ,  $G_2 = 1.2$ . (b) The steerabilities versus  $G_1$ , where  $G_2 = 1.2$ ,  $G_3 = 2$ . (c) The steerabilities versus  $G_1$ , where  $G_2 = 2$ ,  $G_3 = 1.2$ . In subgraph (b) and (c), the solid line and dashed line of the same color correspond to a pair of counterparts, for example, the solid and dashed blue lines correspond to  $\mathcal{G}^{234 \rightarrow 1}$  and  $\mathcal{G}^{1 \rightarrow 234}$ , respectively. (d) Matrix representation diagram when  $G_1 = 3$ ,  $G_2 = 1.2$ ,  $G_3 = 2$ ; (e)  $G_1 = 3$ ,  $G_2 = 2$ ,  $G_3 = 1.2$ .

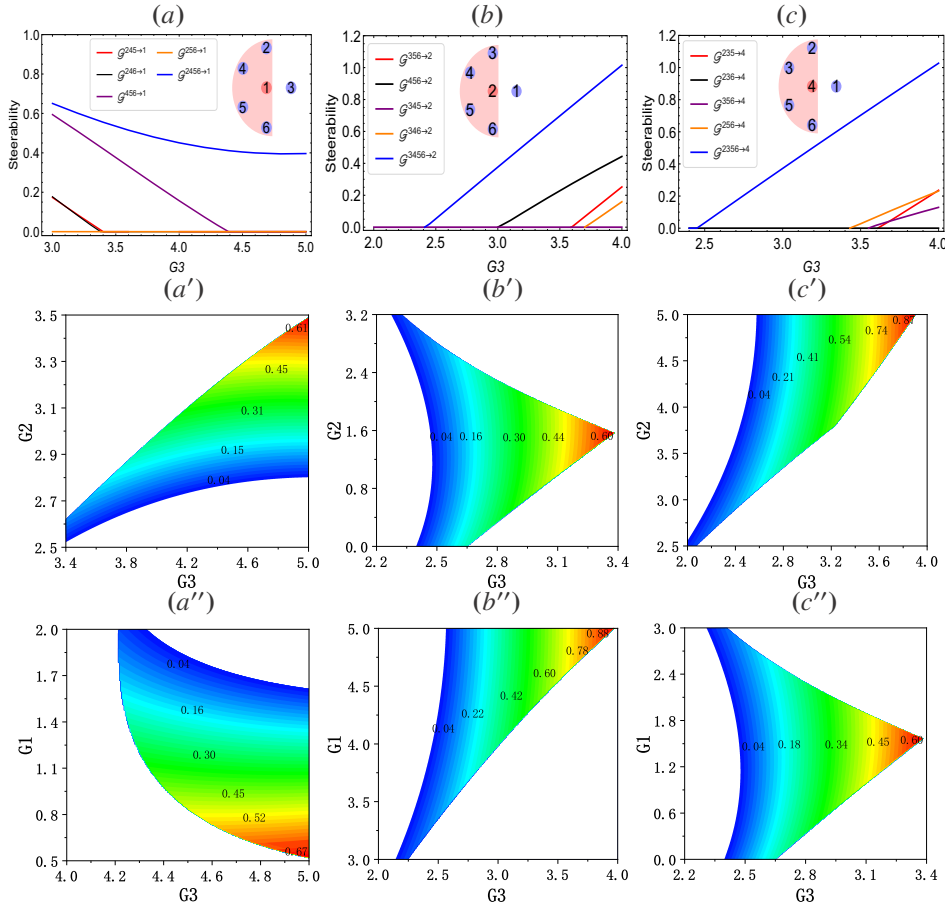
#### 4. Collective multipartite EPR steering

For a quantum system consisting of  $n$  parties, if a given party  $i$  can be steered by all the remaining  $n - 1$  parties, but not by any  $n - 2$  parties, it is called collective multipartite steering. It means that the group of  $n - 1$  parties must collaborate after performing local measurements on each individual system in order to extract the information of party  $i$ , which has potential application to achieve ultra-secure  $n$ -party quantum secret sharing [30,41]. And this kind of special quantum states may provide a solution to the challenges of secure quantum communication network.

Considering a  $n$ -partite case that has one steered mode ( $B$ ) and  $n - 1$  steering modes ( $A_1, A_2, \dots, A_{n-1}$ ), the criterion of the collective multipartite steering can be simplified as [30]

$$\begin{aligned} \mathcal{G}^{A' \rightarrow B} &= 0, & n_{A'} &= n - 2 \\ \mathcal{G}^{A_1 A_2 \dots A_{n-1} \rightarrow B} &> 0, & n_A &= n - 1 \end{aligned} \quad (8)$$

Here  $A'$  includes all  $C_{n-1}^1$  possibilities of one less mode than  $A$  with  $n-1$  mode. It is noticed that only steering party with  $n-1$  modes can steer mode  $B$  but  $n-2$  modes cannot. For six output modes in our model, there exist collective pentapartite steering at most and all its possibilities are shown in STable 1, among which there are three conditions of collective steerings according to three columns, i.e., the two structures in each column have the same steerability, due to the symmetry. It is noticed that mode  $\hat{a}_1$  and  $\hat{a}_3$  cannot be included together in the collective multipartite steerings, which is understandable: if we consider them both, on the one hand, perfect symmetric structure will make it hard to generate collective steering [30]; on the other hand, strong correlations will make steerability of  $n-2$  modes too strong to generate collective steering. Collective pentapartite EPR steering including modes  $(\hat{a}_1\hat{a}_2\hat{a}_4\hat{a}_5\hat{a}_6)$  and  $(\hat{a}_2\hat{a}_3\hat{a}_4\hat{a}_5\hat{a}_6)$  based on the above three conditions are shown in Fig. 6. It is clear in Fig. 6(a), for pentapartite modes  $(\hat{a}_1\hat{a}_2\hat{a}_4\hat{a}_5\hat{a}_6)$ , if  $G_3 > 4.3$  and  $G_1 = 1, G_2 = 3.2$  is chosen, collective steering that only  $\mathcal{G}^{2456 \rightarrow 1}$  can happen and steerings of less steering modes vanish, i.e.,  $\mathcal{G}^{2456 \rightarrow 1} > 0, \mathcal{G}^{256 \rightarrow 1} = \mathcal{G}^{456 \rightarrow 1} = \mathcal{G}^{246 \rightarrow 1} = \mathcal{G}^{245 \rightarrow 1} = 0$ . For pentapartite modes  $(\hat{a}_2\hat{a}_3\hat{a}_4\hat{a}_5\hat{a}_6)$ , if the steered mode is  $\hat{a}_2$  and  $G_1 = 4, G_2 = 2$  is chosen, the collective steering ( $\mathcal{G}^{3456 \rightarrow 2} > 0, \mathcal{G}^{345 \rightarrow 2} = \mathcal{G}^{356 \rightarrow 2} = \mathcal{G}^{346 \rightarrow 2} = \mathcal{G}^{456 \rightarrow 2} = 0$ ) will happen when



**Fig. 6.** Parameter regions of the collective pentapartite steerings including modes  $(\hat{a}_1\hat{a}_2\hat{a}_4\hat{a}_5\hat{a}_6)$  and  $(\hat{a}_2\hat{a}_3\hat{a}_4\hat{a}_5\hat{a}_6)$ . The steered mode in (a)/(a')/(a''), (b)/(b')/(b''), and (c)/(c')/(c'') are  $\hat{a}_1$ ,  $\hat{a}_2$ , and  $\hat{a}_4$ , respectively. The corresponding parameters are: (a)  $G_1 = 1, G_2 = 3.2$ ; (b)  $G_1 = 4, G_2 = 2$ ; (c)  $G_1 = 1.5, G_2 = 4$ . (a'')  $G_1 = 1, (a'')G_2 = 3.2$ ; (b'')  $G_1 = 4; (b'')G_2 = 2$ ; (c'')  $G_1 = 1.5; (c'')G_2 = 4$ .

$2.4 < G_3 < 3.0$ , as is shown in Fig. 6(b). While if the steered mode is  $a_4$  and  $G_1 = 1.5$ ,  $G_2 = 4$  is chosen, the collective steering ( $\mathcal{G}^{2356 \rightarrow 4} > 0$ ,  $\mathcal{G}^{235 \rightarrow 2} = \mathcal{G}^{236 \rightarrow 2} = \mathcal{G}^{356 \rightarrow 2} = \mathcal{G}^{256 \rightarrow 2} = 0$ ) will happen when  $2.45 < G_3 < 3.42$ , as is shown in Fig. 6(c). The parameter range that the collective pentapartite steerings can exist are shown in Fig. 6(a')(b')(c') (collective pentapartite steering versus both  $G_2$  and  $G_3$  when  $G_1$  is fixed) and Fig. 6(a'')(b'')(c'') (collective pentapartite steering versus both  $G_1$  and  $G_3$  when  $G_2$  is fixed). It is worth mentioning that results of Fig. 6(a)/(b)/(c) are included in Fig. 6(a'')(b'')(c'') and Fig. 6(a'')(b'')(c''). For example, in Fig. 6(a'), the parameter range of  $G_2$  and  $G_3$  of the collective pentapartite steering that only  $\mathcal{G}^{2456 \rightarrow 1}$  can happen, is given by the colorful zone, which includes the special condition shown in Fig. 6((a) ( $G_1 = 1$ ,  $G_2 = 3.2$ ,  $G_3 > 4.3$ ). Moreover, as is shown in Fig. 6(a)(a')(a''), for collective steering that only  $\mathcal{G}^{2456 \rightarrow 1}$  can happen, the parameter  $G_3$  should be the strongest to make the original weaker indirect correlation between  $\hat{a}_5, \hat{a}_6$  and  $\hat{a}_1$  strong enough. In the same way, we can also understand that  $G_1$  and  $G_2$  should be the strongest parameter in Fig. 6(b)(b')(b'') and Fig. 6(c)(c')(c''), respectively. Trying to make initial weak correlations strong (make sure steerability of n-1 modes is strong enough) and initial strong correlations weak (make sure steerabilities of n-2 modes are weak to zero) help to build conditions for collective steering. From six parameter regions, it is also noticed that steerabilities that larger than  $\ln(e/2)$  (0.31) can be obtained under proper parameter conditions, therefore it can meet the condition of 1SDI QSS with nonzero key rates [42]. These results mean that one can choose five modes in the output six modes to build a collective pentapartite EPR steering, which includes more modes and have compacter setup, stronger steerabilities, compared with other works.

Table 1. All possible collective steerings

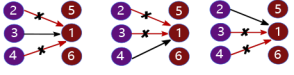
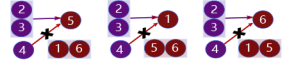
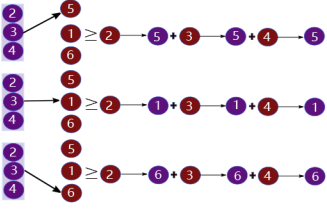
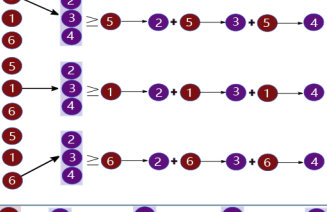

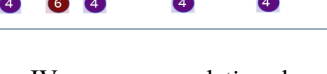

## 5. Monogamy relations

Besides the collective steering, another key point of multipartite steering is the so-called monogamy relations, which is important for understanding how the steerings can be distributed among many parties and has been widely studied both theoretically and experimentally.

There are four types of monogamy relations that have been developed [23,43], for Gaussian states with Gaussian measurements. Considering the six output modes in our model, the four types of monogamy relations are shown in Table 2. As is mentioned in section 3.1, 3.2, and 3.3, all the type-I, type-II, and type-III monogamy relations can be satisfied in our model, which can be found in the corresponding matrix representations. For our six-mode-system, the type-I and type-II monogamy relations mean that the steering parties cannot steer the steered party simultaneously, where the type-I monogamy relations correspond to the condition that all the steering and steered parties include one mode, and the type-II monogamy relations correspond to the condition that the steered party includes one mode and the steering parties include more than one modes, as are shown in the first and second row of Table 2. While the type-III monogamy

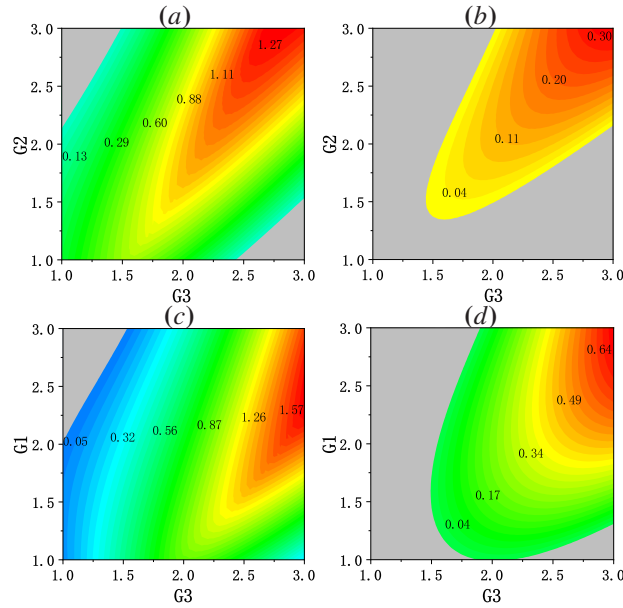
relations mean that the steerability from many modes to one mode is bigger than the sum of that from corresponding one mode to one mode, which can be found in the third row of Table 2. However, the type-IV monogamy relations is about steering from many modes to many modes, and steerability from many modes to many modes is bigger than the sum of steerabilities from corresponding many modes to one mode, or from one mode to many modes.

Table 2. Monogamy Relations

Type	Diagram	Condition
I		$\mathcal{G}^{3 \rightarrow 1} > 0, \mathcal{G}^{2 \rightarrow 1} = 0, \mathcal{G}^{4 \rightarrow 1} = 0$ $\mathcal{G}^{4 \rightarrow 1} > 0, \mathcal{G}^{2 \rightarrow 1} = 0, \mathcal{G}^{3 \rightarrow 1} = 0$ $\mathcal{G}^{2 \rightarrow 1} > 0, \mathcal{G}^{3 \rightarrow 1} = 0, \mathcal{G}^{4 \rightarrow 1} = 0$
II		$\mathcal{G}^{23 \rightarrow 5} > 0, \mathcal{G}^{4 \rightarrow 5} = 0$ $\mathcal{G}^{23 \rightarrow 1} > 0, \mathcal{G}^{4 \rightarrow 1} = 0$ $\mathcal{G}^{23 \rightarrow 6} > 0, \mathcal{G}^{4 \rightarrow 6} = 0$
IIIa		$\mathcal{G}^{234 \rightarrow 5} - \mathcal{G}^{2 \rightarrow 5} - \mathcal{G}^{3 \rightarrow 5} - \mathcal{G}^{4 \rightarrow 5} \geq 0$ $\mathcal{G}^{234 \rightarrow 1} - \mathcal{G}^{2 \rightarrow 1} - \mathcal{G}^{3 \rightarrow 1} - \mathcal{G}^{4 \rightarrow 1} \geq 0$ $\mathcal{G}^{234 \rightarrow 6} - \mathcal{G}^{2 \rightarrow 6} - \mathcal{G}^{3 \rightarrow 6} - \mathcal{G}^{4 \rightarrow 6} \geq 0$
IIIb		$\mathcal{G}^{5 \rightarrow 234} - \mathcal{G}^{5 \rightarrow 2} - \mathcal{G}^{5 \rightarrow 3} - \mathcal{G}^{5 \rightarrow 4} \geq 0$ $\mathcal{G}^{1 \rightarrow 234} - \mathcal{G}^{1 \rightarrow 2} - \mathcal{G}^{1 \rightarrow 3} - \mathcal{G}^{1 \rightarrow 4} \geq 0$ $\mathcal{G}^{6 \rightarrow 234} - \mathcal{G}^{6 \rightarrow 2} - \mathcal{G}^{6 \rightarrow 3} - \mathcal{G}^{6 \rightarrow 4} \geq 0$
IVa		$\mathcal{G}^{156 \rightarrow 234} - \mathcal{G}^{5 \rightarrow 234} - \mathcal{G}^{1 \rightarrow 234} - \mathcal{G}^{6 \rightarrow 234} \geq 0$
IVb		$\mathcal{G}^{234 \rightarrow 156} - \mathcal{G}^{234 \rightarrow 1} - \mathcal{G}^{234 \rightarrow 5} - \mathcal{G}^{234 \rightarrow 6} \geq 0$

Since the type-IV monogamy relations have not been mentioned in the above sections, here we focus on them and mainly discuss about the situation that the steering part and steered part both have three modes, which is naturally included in our model. Considering a quadrupartition system  $(n_A + n_B + n_C + n_D)$ -mode system ABCD, the type-IV monogamy relation can be expressed as  $\mathcal{G}^{D \rightarrow (ABC)} - \mathcal{G}^{D \rightarrow A} - \mathcal{G}^{D \rightarrow B} - \mathcal{G}^{D \rightarrow C} \geq 0$ , or  $\mathcal{G}^{(ABC) \rightarrow D} - \mathcal{G}^{A \rightarrow D} - \mathcal{G}^{B \rightarrow D} - \mathcal{G}^{C \rightarrow D} \geq 0$ , with  $n_A = 1, n_B = 1, n_C = 1, n_D = 3$ . The results of the type-IV monogamy relations, i.e.,  $\mathcal{G}^{156 \rightarrow 234} - \mathcal{G}^{1 \rightarrow 234} - \mathcal{G}^{5 \rightarrow 234} - \mathcal{G}^{6 \rightarrow 234}$ , and  $\mathcal{G}^{234 \rightarrow 156} - \mathcal{G}^{234 \rightarrow 1} - \mathcal{G}^{234 \rightarrow 5} - \mathcal{G}^{234 \rightarrow 6}$ , versus parameters, are shown in Fig. 7(a) and (c) and Fig. 7(b) and (d), respectively. The colorful zones in Fig. 7 correspond to the parameter range that the type-IV monogamy relations can be satisfied, i.e., the type-IV monogamy relations are true or not depend on the parameter conditions, and the lifting of the type-IV monogamy constraint can happen in the grey zone in Fig. 7. It is also noticed that, the bigger the interaction parameter  $G_1, G_2, G_3$ , the bigger the total correlation, the stronger the residual Gaussian steering, which lead to the satisfaction of the type-IV monogamy constraints. From other point of view, the conditional type-IV monogamy relations may provide

the possibility to control the distribution of the steering and may have potential applications in building controllable ultra-secure quantum network.



**Fig. 7.** Parameter regions of type-IV monogamy relation, i.e.,  $\mathcal{G}^{156 \rightarrow 234} - \mathcal{G}^{5 \rightarrow 234} - \mathcal{G}^{1 \rightarrow 234} - \mathcal{G}^{6 \rightarrow 234}$  versus parameters for (a)  $G_1 = 1.2$  and (c)  $G_2 = 2$ .  $\mathcal{G}^{234 \rightarrow 156} - \mathcal{G}^{234 \rightarrow 1} - \mathcal{G}^{234 \rightarrow 5} - \mathcal{G}^{234 \rightarrow 6}$  versus parameters for (b)  $G_1 = 1.2$  and (d)  $G_2 = 2$

## 6. Conclusion

The steering properties of the six output beams that come from the FWM process with SSP have been studied in detail, including the  $(1+i)/(i+1)$ -mode steerings ( $i=1,2,3$ ), the possible collective pentapartite steerings, and the interesting monogamy relations. It is found that the  $(1+i)/(i+1)$  steerings depend on the relative intensity of the related beams and the symmetry of the system, and bigger  $i$  will lead to less parameter dependence. Moreover, collective pentapartite EPR steerings can be obtained with a very compact setup, which are the central resource for ultra-secure hierarchical communication in quantum networks with many users where the issue of trust is of importance. In addition, four types of the monogamy relations are discussed, and only the type-IV monogamy relations are conditional, which provide the possibility to build controllable ultra-secure quantum network. All the results mean that this FWM process with SSP is a promising platform to demonstrate different kinds of EPR steerings and to explore the corresponding valuable applications. By the way, matrix representation is used to express the steerings for the first time, which is not only help to demonstrate all the steerings intuitively, but also very useful in understanding the monogamy relations.

**Funding.** National Key Research and Development Program of China (2021YFA1402002, 2021YFC2201802); National Natural Science Foundation of China (11874248, 11874249, 11974225, 12074233).

**Disclosures.** The authors declare no conflicts of interest.

**Data availability.** Data underlying the results presented in this paper are not publicly available at this time but may be obtained from the authors upon reasonable request.

## References

1. D. M. Greenberger, M. A. Horne, and A. Zeilinger, "Multiparticle interferometry and the superposition principle," *Phys. Today* **46**(8), 22–29 (1993).
2. Z.-A. Jia, R. Zhai, S. Yu, Y.-C. Wu, and G.-C. Guo, "Hierarchy of genuine multipartite quantum correlations," *Quantum Inf. Process.* **19**(12), 419 (2020).
3. R. Uola, A. C. Costa, H. C. Nguyen, and O. Gühne, "Quantum steering," *Rev. Mod. Phys.* **92**(1), 015001 (2020).
4. E. Schrödinger, "Discussion of probability relations between separated systems," in *Mathematical Proceedings of the Cambridge Philosophical Society*, vol. 31 (Cambridge University Press, 1935), pp. 555–563.
5. H. M. Wiseman, S. J. Jones, and A. C. Doherty, "Steering, entanglement, nonlocality, and the einstein-podolsky-rosen paradox," *Phys. Rev. Lett.* **98**(14), 140402 (2007).
6. E. G. Cavalcanti, S. J. Jones, H. M. Wiseman, and M. D. Reid, "Experimental criteria for steering and the einstein-podolsky-rosen paradox," *Phys. Rev. A* **80**(3), 032112 (2009).
7. C. Branciard, E. G. Cavalcanti, S. P. Walborn, V. Scarani, and H. M. Wiseman, "One-sided device-independent quantum key distribution: Security, feasibility, and the connection with steering," *Phys. Rev. A* **85**(1), 010301 (2012).
8. N. Walk, S. Hosseini, J. Geng, O. Thearle, J. Y. Haw, S. Armstrong, S. M. Assad, J. Janousek, T. C. Ralph, T. Symul, H. M. Wiseman, and P. K. Lam, "Experimental demonstration of gaussian protocols for one-sided device-independent quantum key distribution," *Optica* **3**(6), 634–642 (2016).
9. M. Reid, "Signifying quantum benchmarks for qubit teleportation and secure quantum communication using einstein-podolsky-rosen steering inequalities," *Phys. Rev. A* **88**(6), 062338 (2013).
10. Q. He, L. Rosales-Zárate, G. Adesso, and M. D. Reid, "Secure continuous variable teleportation and einstein-podolsky-rosen steering," *Phys. Rev. Lett.* **115**(18), 180502 (2015).
11. M. Piani and J. Watrous, "Necessary and sufficient quantum information characterization of einstein-podolsky-rosen steering," *Phys. Rev. Lett.* **114**(6), 060404 (2015).
12. S. Midgley, A. Ferris, and M. Olsen, "Asymmetric gaussian steering: when alice and bob disagree," *Phys. Rev. A* **81**(2), 022101 (2010).
13. V. Händchen, T. Eberle, S. Steinlechner, A. Samblowski, T. Franz, R. F. Werner, and R. Schnabel, "Observation of one-way einstein-podolsky-rosen steering," *Nat. Photonics* **6**(9), 596–599 (2012).
14. E. Cavalcanti, Q. He, M. Reid, and H. Wiseman, "Unified criteria for multipartite quantum nonlocality," *Phys. Rev. A* **84**(3), 032115 (2011).
15. Q. Y. He and M. D. Reid, "Genuine multipartite einstein-podolsky-rosen steering," *Phys. Rev. Lett.* **111**(25), 250403 (2013).
16. S. Armstrong, M. Wang, R. Y. Teh, Q. Gong, Q. He, J. Janousek, H.-A. Bachor, M. D. Reid, and P. K. Lam, "Multipartite einstein-podolsky-rosen steering and genuine tripartite entanglement with optical networks," *Nat. Phys.* **11**(2), 167–172 (2015).
17. J. Li and S.-Y. Zhu, "Einstein-podolsky-rosen steering and bell nonlocality of two macroscopic mechanical oscillators in optomechanical systems," *Phys. Rev. A* **96**(6), 062115 (2017).
18. H. Tan and J. Li, "Einstein-podolsky-rosen entanglement and asymmetric steering between distant macroscopic mechanical and magnonic systems," *Phys. Rev. Res.* **3**(1), 013192 (2021).
19. Q. He and M. Reid, "Einstein-podolsky-rosen paradox and quantum steering in pulsed optomechanics," *Phys. Rev. A* **88**(5), 052121 (2013).
20. X. Deng, Y. Xiang, C. Tian, G. Adesso, Q. He, Q. Gong, X. Su, C. Xie, and K. Peng, "Demonstration of monogamy relations for einstein-podolsky-rosen steering in gaussian cluster states," *Phys. Rev. Lett.* **118**(23), 230501 (2017).
21. Y. Cai, Y. Xiang, Y. Liu, Q. He, and N. Treps, "Versatile multipartite einstein-podolsky-rosen steering via a quantum frequency comb," *Phys. Rev. Res.* **2**(3), 032046 (2020).
22. H. Wang, C. Fabre, and J. Jing, "Single-step fabrication of scalable multimode quantum resources using four-wave mixing with a spatially structured pump," *Phys. Rev. A* **95**(5), 051802 (2017).
23. Y. Xiang, Y. Liu, Y. Cai, F. Li, Y. Zhang, and Q. He, "Monogamy relations within quadripartite einstein-podolsky-rosen steering based on cascaded four-wave mixing processes," *Phys. Rev. A* **101**(5), 053834 (2020).
24. S. Kim and A. M. Marino, "Atomic resonant single-mode squeezed light from four-wave mixing through feedforward," *Opt. Lett.* **44**(19), 4630–4633 (2019).
25. V. Boyer, A. M. Marino, R. C. Pooser, and P. D. Lett, "Entangled images from four-wave mixing," *Science* **321**(5888), 544–547 (2008).
26. R. Ma, W. Liu, Z. Qin, X. Su, X. Jia, J. Zhang, and J. Gao, "Compact sub-kilohertz low-frequency quantum light source based on four-wave mixing in cesium vapor," *Opt. Lett.* **43**(6), 1243–1246 (2018).
27. Z. Qin, L. Cao, H. Wang, A. Marino, W. Zhang, and J. Jing, "Experimental generation of multiple quantum correlated beams from hot rubidium vapor," *Phys. Rev. Lett.* **113**(2), 023602 (2014).
28. W. Wang, L. Cao, Y. Lou, J. Du, and J. Jing, "Experimental characterization of pairwise correlations from triple quantum correlated beams generated by cascaded four-wave mixing processes," *Appl. Phys. Lett.* **112**(3), 034101 (2018).
29. Y. Liu, Y. Cai, Y. Xiang, F. Li, Y. Zhang, and Q. He, "Tripartite einstein-podolsky-rosen steering with linear and nonlinear beamsplitters in four-wave mixing of rubidium atoms," *Opt. Express* **27**(23), 33070–33079 (2019).
30. Y. Liu, Y. Cai, B. Luo, J. Yan, M. Niu, F. Li, and Y. Zhang, "Collective multipartite einstein-podolsky-rosen steering via cascaded four-wave mixing of rubidium atoms," *Phys. Rev. A* **104**(3), 033704 (2021).

31. K. Zhang, W. Wang, S. Liu, X. Pan, J. Du, Y. Lou, S. Yu, S. Lv, N. Treps, C. Fabre, and J. Jing, "Reconfigurable hexapartite entanglement by spatially multiplexed four-wave mixing processes," *Phys. Rev. Lett.* **124**(9), 090501 (2020).
32. A. Dong, K. Zhang, and J. Jing, "Generation of twelve-partite entanglement from two symmetric four-wave mixing processes," *Opt. Commun.* **521**, 128470 (2022).
33. W. Wang, K. Zhang, and J. Jing, "Large-scale quantum network over 66 orbital angular momentum optical modes," *Phys. Rev. Lett.* **125**(14), 140501 (2020).
34. J. D. Swaim, E. M. Knutson, O. Danaci, and R. T. Glasser, "Multimode four-wave mixing with a spatially structured pump," *Opt. Lett.* **43**(11), 2716–2719 (2018).
35. S. Liu, H. Wang, and J. Jing, "Two-beam pumped cascaded four-wave-mixing process for producing multiple-beam quantum correlation," *Phys. Rev. A* **97**(4), 043846 (2018).
36. S. Liu, Y. Lou, and J. Jing, "Experimental characterization of multiple quantum correlated beams in two-beam pumped cascaded four-wave mixing process," *Opt. Express* **27**(26), 37999–38005 (2019).
37. H. Wang, K. Zhang, N. Treps, C. Fabre, J. Zhang, and J. Jing, "Generation of hexapartite entanglement in a four-wave-mixing process with a spatially structured pump: Theoretical study," *Phys. Rev. A* **102**(2), 022417 (2020).
38. N. C. Menicucci, S. T. Flammia, and P. van Loock, "Graphical calculus for gaussian pure states," *Phys. Rev. A* **83**(4), 042335 (2011).
39. X. Zhu, C.-H. Chang, C. González-Arciniegas, A. Pe'er, J. Higgins, and O. Pfister, "Hypercubic cluster states in the phase-modulated quantum optical frequency comb," *Optica* **8**(3), 281–290 (2021).
40. I. Kogias, A. R. Lee, S. Ragy, and G. Adesso, "Quantification of gaussian quantum steering," *Phys. Rev. Lett.* **114**(6), 060403 (2015).
41. M. Wang, Q. Gong, and Q. He, "Collective multipartite einstein–podolsky–rosen steering: more secure optical networks," *Opt. Lett.* **39**(23), 6703–6706 (2014).
42. Y. Xiang, I. Kogias, G. Adesso, and Q. He, "Multipartite gaussian steering: Monogamy constraints and quantum cryptography applications," *Phys. Rev. A* **95**(1), 010101 (2017).
43. M. D. Reid, "Monogamy inequalities for the einstein–podolsky–rosen paradox and quantum steering," *Phys. Rev. A* **88**(6), 062108 (2013).